Journal of Basic and Applied Engineering Research
p-ISSN: 2350-0077; e-ISSN: 2350-0255; Volume 3, Issue 11; July-September, 2016, pp. 1004-1009

http://www.krishisanskriti.org/Publication.html

Pseudoplastic Fluid Flow around a Square Cylinder with a Downstream Splitter Plate

Babli Varsha[1], Sudipto Sarkar[2] and Anamika Paul[3]

[1]Graduate student, School of Chemical Engineering, Galgotias University, India
[2]School of Mechanical Engineering, Galgotias University, India
[3]School of Chemical Engineering, Galgotias University, India
E-mail: [2]sudipto.sarkar@galgotiasuniversity.edu.in

Abstract—*Two-dimensional simulation of non-Newtonian fluid (Pseudoplastic in nature) flow over a square cylinder with a thin downstream splitter plate is carried out to control the vortex shedding from the cylinder using Ansys Fluent. The research is conducted for three different gap-ratios (G/a = 2, 2.25 and 2.5, where G is the gap between cylinder and plate and a is length of the side of the cylinder) considering fluid with three different flow behavior indices (n =1, 0.8 and 0.5). Instantaneous flow visualization along with aerodynamic forces are presented to understand the changes associated with vortex suppression in non-Newtonian environment. It has been observed that at very low value of n (n = 0.5) the vortex shedding process differ drastically from the Newtonian flow cases.*

1. INTRODUCTION

In the last few decades, research in the field of passive flow control has shown that a splitter plate set along the bluff body wake centerline reduces drag and may inhibit vortex shedding [1, 2]. For a Reynolds number of 1.45×10^4, Roshko [3] was notably one of the first to report periodic vortex formation suppression using a circular cylinder connected with a splitter plate. He also showed that, by positioning this splitter plate at different fixed distances in the fully developed cylinder-wake, the Strouhal number ($St = fD/U_\infty$, where f is the frequency of vortex shedding, D is the diameter of the cylinder and U_∞ is the free-stream velocity) diminishes as the distance between the cylinder and the plate increases up to a limit position $G \approx 2.7D$.

Apelt et al. [4] and Apelt & West [5] carried out experiments with two combinations, a circular cylinder connected with a splitter plate and a normal flat plate (fixed separation points) connected with a splitter plate, to show the influence of the splitter plate length ($0 < l < 7$) on drag and vortex shedding ($10^4 \leq Re \leq 5\times10^4$). They concluded that short splitter plate lengths ($l \leq 2$) can significantly change the characteristics of the downstream flow from both the circular cylinder and the normal flat plate. They also established that splitter plates longer than $2D$ decrease the drag and progressively slow the vortex shedding until $l = 3D$ for the flat plate and $l = 5D$ for the circular cylinder. Beyond these splitter plate lengths, no further change occurs, the drag coefficient C_D remains constant and the vortex shedding ceases. Each of these steady flow studies showed that a splitter plate was an efficient means of passive control in a fully developed wake.

Ali et al. [6] simulated wake flow from a square cylinder interacted with a splitter plate at $Re = 150$. Sensitivity of near wake flow structure to the downstream position of plate is investigated at varying gap ratios ($0 < G/D < 7$) for a constant plate length. Two flow regimes were identified with the transition at critical gap distance $G_C \approx 2.3D$. The first regime was characterized by the completion of vortex formation in the downstream of the gap and the second regime as completion of vortex formation within the gap. The authors also observed that the splitter plate had no effect on the generation of Kármán vortex when the gap is beyond $5.6D$.

Srivastava and Sarkar [7] in their simulation kept a splitter plate behind a square cylinder and vary the gap-ratio up to $G/a = 2$ (below G_{cr}) at $Re = 100$. The authors proposed to divide the inner region of critical gap in another two sub-regions due to the difference in flow physics before and after $G/a = 1$. Jain et al. [8] considered the same flow domain and Re, but performed their simulation for $G/a = 2.5 – 4$. They observed that as the gap-ratio increased, the vortex roll-up started in the intermediate region between the cylinder and splitter plate.

From these literature reviews it can be concluded that almost all works in controlling of vortex shedding using splitter plate have been carried out considering Newtonian flow environment, although in process industries and chemical industries a large number of fluids are used which are non-Newtonian in nature. Keeping this in view, in the present work authors simulate the wake-control problem considering the nature of the fluid as pseudoplastic (n < 1) and evaluate the differences in flow field with Newtonian flow (n = 1).

2. NUMERICAL METHODS

2.1 Governing Equations

Fluids are classified as having Newtonian and non-Newtonian behavior, depending on whether they can be described by

Newton's law of viscosity or not. Further non-Newtonian fluids in which rheological behavior depends only on the shear stress (at constant temperature) are considered as time-independent. The shear stress τ of these kind of fluids can be expressed in power-law form $\tau = K\left(\frac{\partial u}{\partial y}\right)^n$, where K is the flow consistency index and $\frac{\partial u}{\partial y}$ is the velocity gradient perpendicular to the plane of shear. The generalized Navier-Stokes equations are used for momentum considering the shear stress obtained from above equation.

2.2 Computational details

The geometry of the flow domain is developed using Gambit 2.2.30, which also helps to impose the boundary conditions. The coordinates x and y denote the streamwise and wall-normal directions respectively and the corresponding velocities are denoted by u and v. Cartesian grid is used for the simulation considering the origin of the axes lie at the cylinder's downstream face centre.

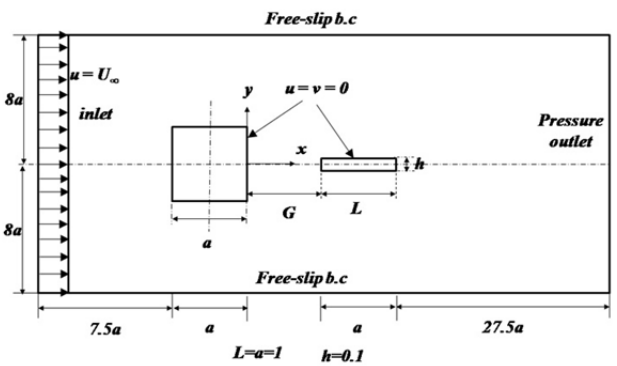

Figure 1: Schematic diagram of flow geometry along with boundary conditions

Figure 1 represents the schematic diagram of flow geometry along with the boundary conditions. The origin of the axes is also included in the figure. The computational domain extends up to -8.5a at the inflow and ±8a in flow normal directions from the origin and 27.5a in the outflow from the trailing edge of the flat plate for all cases. Here the boundary conditions are set by considering velocity inlet (u = U_∞), pressure outlet, symmetry (free-slip boundary condition) at upper and lower domain. Wall boundary condition (u = v = 0) is imposed both on the cylinder and the splitter plate surfaces. Since the flow is purely one dimensional, hence flow exists only in x direction, where velocity inlet boundary condition is used to define the flow velocity at the flow inlet, i.e., u = 1, v = w = 0. The Navier-Stokes (momentum) equation is non-dimensionalized by considering a and U∞ as unity. The flow field is then solved by Ansys Fluent 14.5 using SIMPLE algorithm in second-order upwind momentum scheme with a standard pressure solver. A total of 20 iterations at each time step are considered to increase the accuracy of the solution.

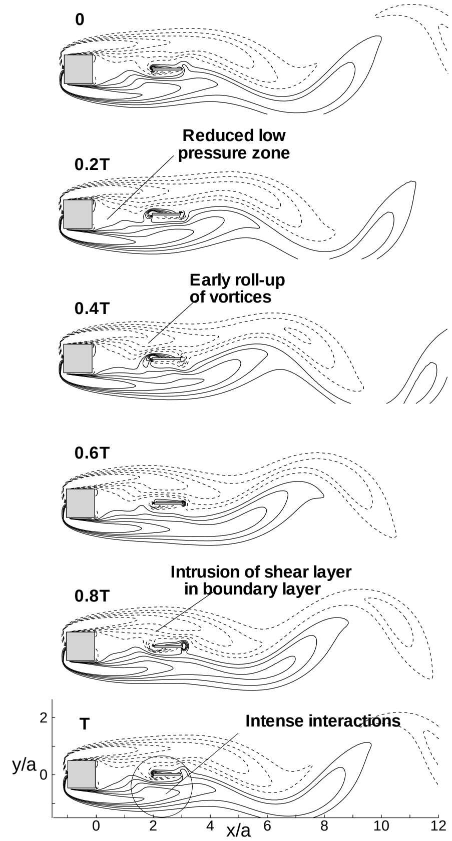

Figure 2: Instantaneous vorticity contours for *G/a* =2 and *n* = 1.

A mesh of 268×208 points in the streamwise and flow normal directions are used for G/a = 0 after performing a grid independent test for a square cylinder in an unbounded condition [7]. For the present simulation, a total of 316×208, 322×208 and 328×208 grid points are used for G/a = 2, 2.25 and 2.5 respectively. The increase in total number of grid points in streamwise direction with high G/a is directly related with the increase of domain size in that direction. Also similar kind of grid distribution was considered by Pal and Sarkar [9] and Raees and Sarkar [10] in their work at Re = 100.

3. RESULTS AND DISCUSSION

To understand the effect of pseudoplastic fluid flow in wake control, total 9 cases have been considered by varying gap-ratio (G/a = 2, 2.25 and 2.5) and flow behavior index (n = 1, 0.8, 0.5). It should be noted that n = 0.8 and n = 0.5 cases belong to pseudoplastic flow, whereas, n = 1 is for Newtonian fluid flow.

The Instantaneous spanwise vorticity, ω_z has been depicted in Figures 2 - 6 for five different cases. Total six frames has been considered for each Figure and those frames have been drawn in a single time period (T) at equal time intervals (t/T = 0. 0.2, 0.4, 0.6, 0.8 & 1). The value of T is decided from the flow evolution of the present problem such that after completion of a time period almost exact instantaneous flow field is obtained. For every time frame total 10 contours are considered in between $\omega_z = \pm 1$ (non- dimensional values) and negative contours are shown by dotted lines to differentiate them with positive ones.

Figure 2 represents ω_z contours for G/a = 2 and n = 1 (Newtonian fluid). From the figure it has been observed that high stretching of upper and lower shear layer formed behind the cylinder which can be attributed to a presence of downstream splitter plate which restricts the vortex formation close to the cylinder. It also illustrates the negative pressure zone just after the cylinder is of low intensity as compared to an unbounded cylinder. The boundary layer formed over the splitter plate is highly disturbed due to extension of shear layer into it. Also, a high interaction between cylinder shear layer and splitter plate boundary can be observed from the instantaneous portraits.

As the value of n reduces, the stretching of cylinder shear layers also reduces which can clearly be seen from Fig. 3 (G/a = 2 and n = 0.5). As the shear layers now try to roll very close to cylinder, the interaction of them (shear layers) with the plate boundary layer becomes more significant and the intensity of the interaction is quite high as compared to the first case. The low pressure zone behind the cylinder is almost negligible and in the far field of the flow domain. Proper Kármán like vortex shedding is obtained only after x/a = 8.

For intermediate gap-ratio (G/a = 2.25), no results are included for n = 1, 0.8 as they have only minute differences from G/a = 2. At this gap, the flow visualization of highly pseudoplastic flow (n = 0.5) reflect very high interaction of shear layers with the splitter plate boundary layer (refer Fig. 4) which may lead to the transition of flow. At critical gap-ratio

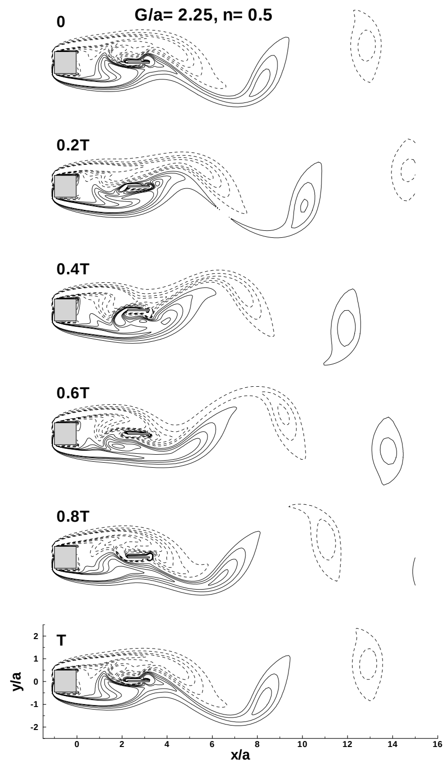

Figure 3: Instantaneous vorticity contours for *G/a* =2 and *n* = 0.5.

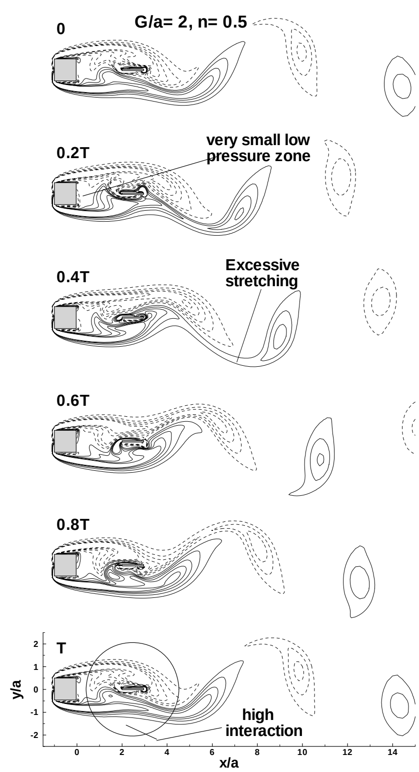

Figure 4: Instantaneous vorticity contours for *G/a* =2.25 and *n* = 0.5.

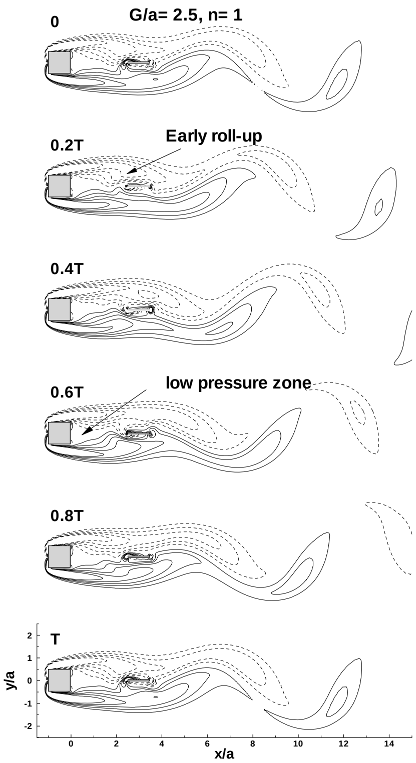

Figure 5: Instantaneous vorticity contours for *G/a* =2.5 and *n* = 1.

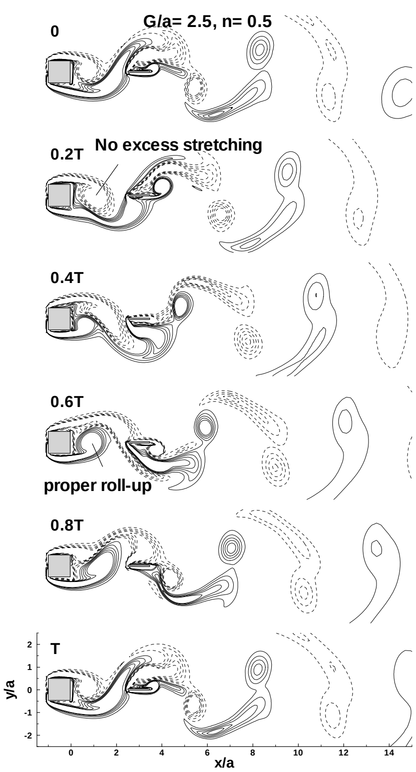

Figure 6: Instantaneous vorticity contours for *G/a* =2.5 and *n* = 0.5.

(G/a = 2.5), instantaneous vorticity results for all three values of n (n = 1, 0.8 and 0.5) are depicted in Figs. 4 - 6 due to some interesting features of the flow field. As expected very high interaction near the plate is observed at n = 1 and 0.8 (Figs. 4 & 5 respectively) that clearly indicate the change of flow physics. It should be mentioned here that the critical gap ratio remains unaffected at n = 0.8.

Interesting difference particularly in case of G/a = 2.5 and n = 0.5 is observed in instantaneous vorticity diagram (Fig. 6). For this case, the shear layers from the cylinder are not stretched up to the splitter plate but they roll-up early and produce vortices in between the cylinder and splitter plate. This difference in the position of vortex formation changes the flow dynamics completely for this particular case. A remarkable conclusion can be made from here: the critical gap-ratio for pseudoplastic fluid flow at n = 0.5 is not closed to 2.5, but it is in between 2 and 2.5. This means as the nature of flow changes from Newtonian to pseudoplastic the critical gap-ratio reduces (moves towards upstream) and vortex formation start as early as expected in case of Newtonian flow. These vortices also interact with the boundary layers formed on both sides of flat plate and therefore a highly interactive flow field is observed after the splitter plate.

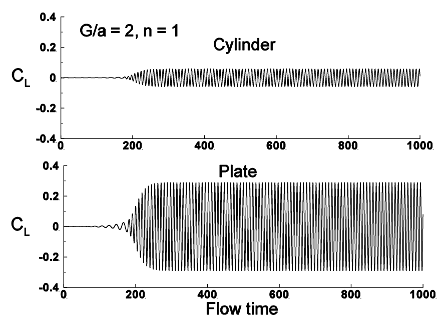

(a)

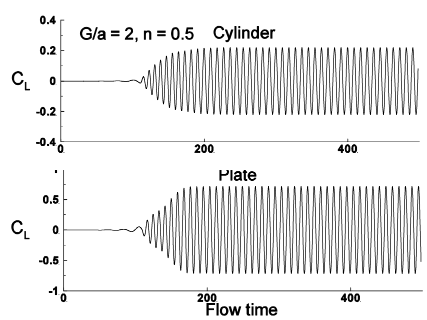

(b)

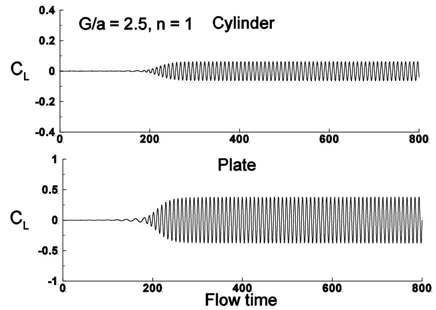

(c)

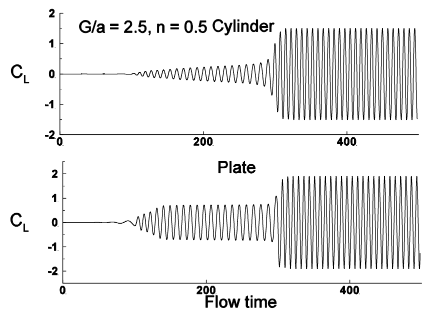

(d)

Figure 7: Time evolution of C_L both for cylinder and plate. (a) *G/a* = 2, *n* = 1; (b) *G/a* = 2, *n* = 0.5; (c) *G/a* = 2.5, *n* = 1; (d) *G/a* = 2.5, *n* = 0.5.

Table 1: Few mean flow parameters related with the present study. Notations used contain usual meaning.

Case	*G/a*	*n*	$\overline{C_D}$	$\overline{c_{p_b}}$	L_r/a
1.	2	1	1.432	-0.533	3.820
2.	2	0.8	1.393	-0.559	3.460
3.	2	0.5	1.479	-0.660	3.233
4.	2.25	1	1.429	-0.530	3.781
5.	2.25	0.8	1.388	-0.555	3.262
6.	2.25	0.5	1.461	-0.640	3.400
7.	2.5	1	1.427	-0.527	3.896
8.	2.5	0.8	1.384	-0.550	3.789
9.	2.5	0.5	1.479	-0.943	1.903

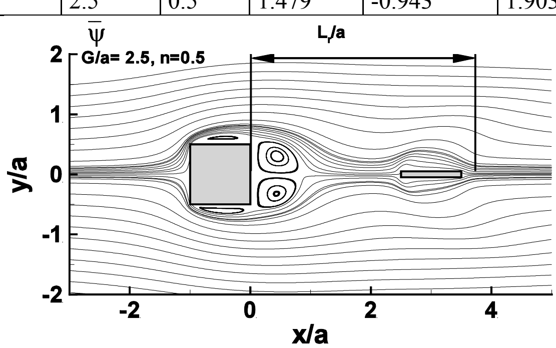

(a)

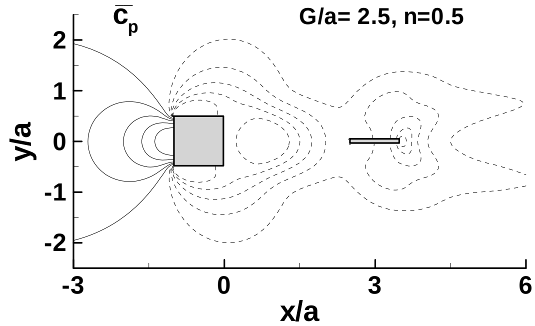

(b)

Figure 8: Time averaged contours at *G/a* = 2.5 and *n* = 0.5: (a) streamlines, (b) C_p.

The time evolution of aerodynamic lift force coefficient ($C_L = \frac{F_L}{\frac{1}{2}\rho U_\infty^2 a}$, where F_L is the lift force) is depicted both for cylinder and plate in Fig. 7. For all cases at the beginning (up to 200 non-dimensional flow time) there is no variation in the values of C_L. This can be attributed to the fact that the flow needs significant time to develop. After the flow is developed, a periodic variation of C_L value is observed which is due to the start of vortex shedding in the flow field. Also it can be seen from Fig. 7 that the range of C_L value enhances drastically as the fluid nature changes from Newtonian to pseudoplastic. This can be attributed to an unsuppressed vortex shedding for pseudoplastic flow (n = 0.5).

For a quantitative analysis of all flow cases at different gap-ratios, Table 1 is included in the result section which comprises of the time-averaged quantities like mean drag coefficient ($\overline{C_D} = \frac{1}{T}\int_0^T C_D$, where $C_D = \frac{F_D}{\frac{1}{2}\rho U_\infty^2 a}$, F_D is the drag force), back pressure coefficient ($C_{Pb} = \frac{P_b - P_\infty}{\frac{1}{2}\rho U_\infty^2}$, where P_b is the back pressure at rear stagnation point of the cylinder) and bubble-recirculation length (L_r). It can be concluded that the range of variation of C_D is quite low as compared to C_L both for the cylinder and plate. The mean value of lift and drag coefficient ($\overline{C_L}$ and $\overline{C_D}$), their maximum and minimum values and ranges are tabulated for all cases in Table.-1. Also the back pressure coefficient (C_{pb}) values are given in the same Table for better understanding of flow physics. It is observed from the Table that as n reduces from 1 to 0.8, the $\overline{C_D}$ value of cylinder also reduces but when n value changes from 0.8 to 0.5 there is an increase of $\overline{C_D}$value. This difference in $\overline{C_D}$ open the door to finding the optimal value of n for which $\overline{C_D}$ is minimum.The negative value of C_{pb} can be attributed to the negative pressure behind the cylinder and the magnitude increases with the decrease of n value and increase of G/a. The lowest value of $L_r/a,$ at n = 0.5, is associated with low separation region and early vortex formation.

The time averaged streamlines and mean pressure coefficient are illustrated in Fig. 8 for a particular case G/a = 2.5 and n = 0.5. Time averaging of the flow variables has been done considering five non-dimensional time periods. Similar to instantaneous flow field, here also the early roll-up and breakdown of vortices in case of highly pseudoplastic flow was observed. This finding is remarkable because it confirms the shifting of critical gap-ratio towards cylinder in case of psudoplastic flow as compared to Newtonian one.

4. CONCLUSIONS

Passive control of vortices using splitter plate downstream of the cylinder is simulated using Ansys Fluent for a low Reynolds number (Re = 100) within the critical gap ratio. Different fluids (n = 1, 0.8 and 0.5) are used in this study to see the effect of splitter plate to control the vortices and reduction of drag forces.

The following major findings are listed below:

a) The instantaneous flow field illustrates that for Newtonian flow (n = 1) the stretching of shear layer is very high and extends up to the splitter plate.
b) As the value of n reduces (n = 0.8, 0.5 for pseudoplastic flow), the stretching of shear layer also reduces and try to roll up before the plate. Therefore the interaction of the shear layer with the splitter plate boundary layer is very high.
c) Similar kind of physics is observed in case of G/a = 2.25 and 2.5 as in a) and b) above.
d) The mean drag coefficient $\overline{C_D}$ is minimum at G/a = 2.5 for n = 1 and n = 0.8. This concludes that the critical gap ratio for both the n values lie close to G/a = 2.5.
e) However, for highly Pseudoplastic flow (n = 0.5), the minimum value of $\overline{C_D}$ is observed at G/a = 2.25 ($\overline{C_D}$= 1.461) instead of at G/a = 2.5. From here it can be concluded that as the nature of flow changes from Newtonian to Pseudoplastic, the critical gap ratio also reduces.

REFERENCES

[1] Monkewitz, P. A., Eckelman, H., Graam, J. M. R, Huerre, P., Wake control in Bluff Body Wakes, Dynamics and Instabilities, I.U.T.A.M. Symposium Gottingen, Springer, Germany, 1992, pp. 227 - 240.

[2] Fiedler, H. E., Fernholz, H. H., On management and control of turbulent shear flows, Prog. Aerospace Sci. 27 (1990) 305 - 387.

[3] Roshko, A., On the drag and shedding frequency of two dimensional bluff bodies, National advisory committee for aeronautics, Technical Note 3169, 1954, pp. 1 - 29.

[4] Apelt, C. J., West, G. S., Szewczyk, A., The effects of wake splitter plates on the ¯ow past a circular cylinder in the range $10^4 < Re < 5\times10^4$, J. Fluid Mech., 61, 1973, pp. 187 - 198.

[5] Apelt, C. J., West, G. S., The effects of wake splitter plates on bluff body flow in the range $10^4 < Re < 5\times10^4$, part 2, J. Fluid Mech. ,71, 1975, 145-160.

[6] Ali, M. S. M., Doolan, C. J., and Wheatley, V., "Low Reynolds number flow over a square cylinder with a splitter plate", *Physics of Fluids*, 23, 2011, 033602 (12 pp.).

[7] Srivastava, S., and Sarkar, S., "Wake interaction of a square cylinder with a splitter plate boundary layer at a low Reynolds number*", AJK2015-FED*, Seoul, 2015, AJKFluids2015-01793 (6 pages).

[8] Jain, S., Sharma, S., and Sarkar, S., "Low Reynolds number flow over a square cylinder in vicinity of a downstream splitter plate", *Journal of Material Science and Mechanical Engineering*, 13(2), 2015, pp. 77-81.

[9] Pal, A., and Sarkar, S., "Wake-Boundary Layer Interactions behind a Square Cylinder for a Reynolds number in Periodic Vortex Shedding Regime*", AJK2015-FED*, Seoul, 2015, AJKFluids2015-01794 (6 pages).

[10] Raees, M., and Sarkar, S., "Wake-wake interactions for a pair of staggered cylinders at a low Reynolds Number (Re = 100)*", AJK2015-FED*, Seoul, 2015, AJKFluids2015-01795 (6 pages).